Probabilistic Calibration of a Closed-loop Cardiac Electromechanical Model with Application to Cardiac Resynchronization Therapy
Supplementary Material

Ester Bergantin[1], Federica Caforio[2,3,4], Francisco Sahli Costabal[5,6,7], Christoph M. Augustin[3,4], and Simone Pezzuto*[1,8]

[1]Laboratory of Mathematics for Biology and Medicine, Department of Mathematics, University of Trento, Italy
[2]Department of Mathematics and Scientific Computing, NAWI Graz, University of Graz, Austria
[3]Gottfried Schatz Research Center, Division of Medical Physics and Biophysics, Medical University of Graz, Austria
[4]BioTechMed-Graz, Austria
[5]Department of Mechanical and Metallurgical Engineering, School of Engineering, Pontificia Universidad Católica de Chile, Chile
[6]Institute for Biological and Medical Engineering, Schools of Engineering, Medicine and Biological Sciences, Pontificia Universidad Católica de Chile, Chile
[7]Millennium Institute for Intelligent Healthcare Engineering, iHEALTH, Chile
[8]Euler Institute, Università della Svizzera italiana, Switzerland

A Bayesian Optimization iterations

For the Bayesian optimization we had to select the number of steps for the optimization. Ideally, the number of steps for the optimization should be as high as possible, which allows a better knowledge of the function and its minimum, however, as it increases, the computational cost also increases. Then, the task is to balance both aspects. In this work we perform the optimization for 300 steps. To evaluate the chosen optimization budget, Figure S1 illustrates the convergence behavior of the loss function across the iterations for the patient cohort. The running minimum of the loss function (orange line) consistently reaches a stable plateau well before the maximum iteration limit. Specifically, the global optimum is identified at iteration 231 for Patient 1, 223 for Patient 2, 93 for Patient 3, and 253 for Patient 4. This behavior demonstrates that a budget of 300 iterations provides a robust margin for accurate parameter identification while maintaining computational efficiency.

B AHA regions

The LV free wall (LVfw) and the interventricular septum (IVS) were subdivided according to the 16-region AHA segmentation [1]. The LVfw comprises 11 segments (4 basal, 4 medial, and 3 apical), while the IVS comprises 5 segments (2 basal, 2 medial, and 1 apical). For the RV free wall (RVfw), three longitudinal bands (basal, medial, and apical) were defined, with 3 circumferential divisions (anterior, lateral, inferior) in the basal and medial bands and 2 in the apical band.

The regions were defined using the universal ventricular coordinates (UVC) introduced in [2], which provide a global positioning system for three-dimensional biventricular geometries through four scalar fields: apicobasal, transmural, rotational, and transventricular coordinates, each obtained as the solution of a Laplace problem. In this work, the transmural coordinate was not required.

Figure S2 illustrates the three coordinates used to define the AHA regions on a patient-specific biventricular geometry, together with the corresponding bullseye representation. The transventricular coordinate (Fig. S2A) distinguishes between the LV (blue cavity) and RV (purple cavity).

The apicobasal coordinate $\mathfrak{z}$ (Fig. S2B), defined in $[0, 1]$, represents the normalized distance along the ventricular long axis from apex to base. To ensure a smooth and uniform variation of $\mathfrak{z}$, the geodesic

*Corresponding author. E-mail: simone.pezzuto@unitn.it

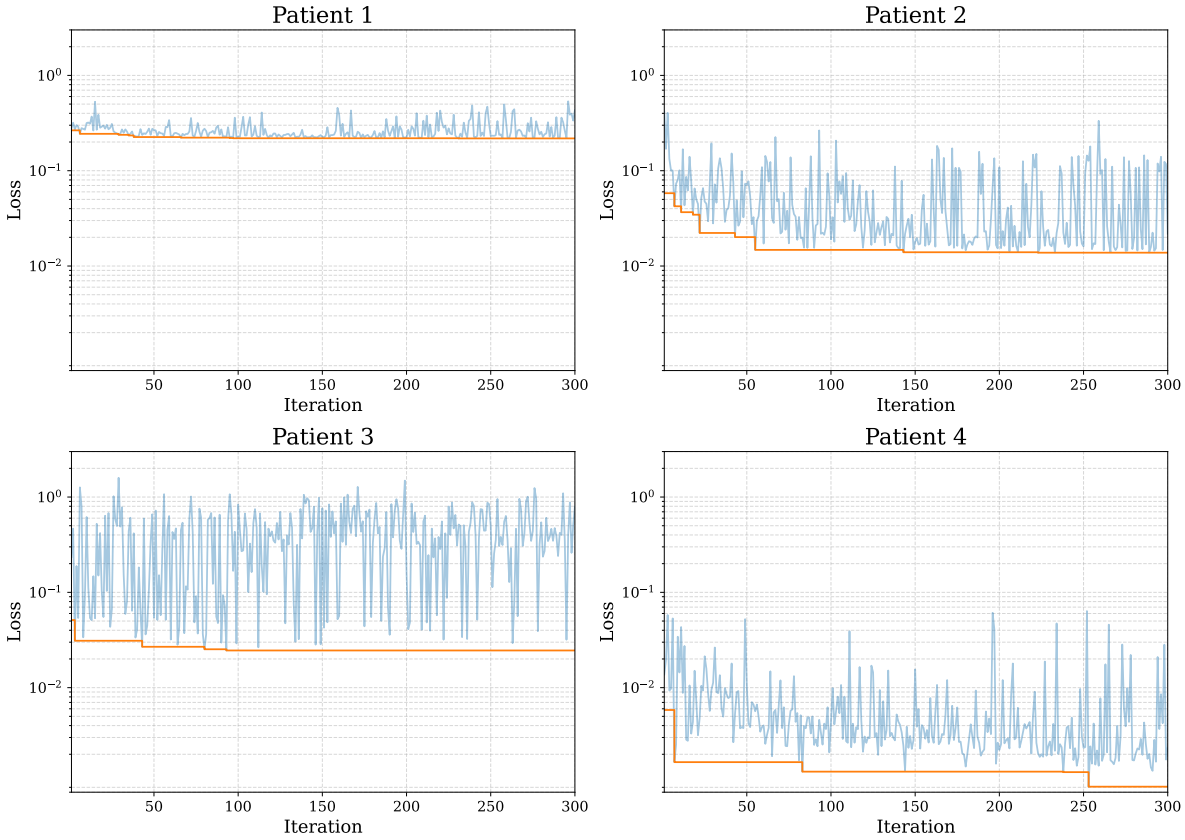

Figure S1: Loss function over the 300 iterations of Bayesian optimization. The orange line represents the minimum value reached up to that number of iterations, while the blue line shows the value of the loss function of the acquired sample at each iteration.

normalization approach proposed in [3] was employed. Specifically, the shortest geodesic path from apex to base was computed, and the initial Laplace solution was reparameterized along this path as a function of normalized distance.

The basal, medial, and apical regions were defined by partitioning the interval $[0, 1]$ into three equal segments, corresponding to $\mathfrak{z} < \frac{1}{3}$, $\frac{1}{3} \leq \mathfrak{z} < \frac{2}{3}$, and $\mathfrak{z} \geq \frac{2}{3}$, respectively.

The rotational coordinate (Fig. S2C), defined in $[-\pi, \pi]$, represents the circumferential position around the ventricular long axis. Circumferential sectors were obtained by partitioning this interval into sub-intervals corresponding to the desired number of regions and assigning nodes based on their rotational coordinate. The stars in the bullseye representation indicate the regions corresponding to the IVS.

The activation time for each region was defined as the mean electrical activation time over all nodes within that region. In the following, each region is referred to as a *patch*.

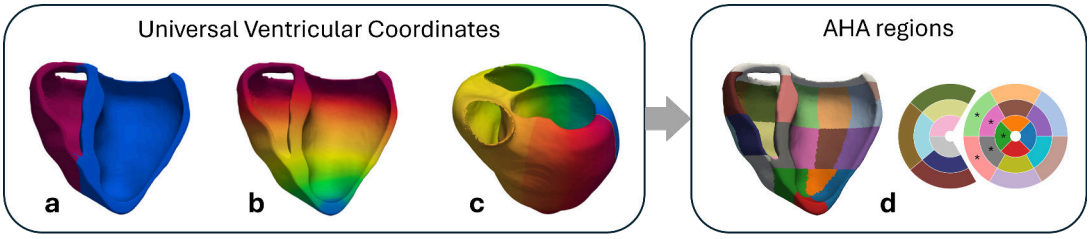

Figure S2: UVC on a patient-specific biventricular geometry to define AHA regions. **a**: transventricular coordinate, **b**: apicobasal coordinate, **c**: rotational coordinate. **d**: AHA regions are represented in bullseye form, where the stars indicate the IVS.

C CircAdapt modules

In this appendix, we summarize the main governing equations of the CircAdapt model. Before introducing the MultiPatch formulation, we first describe the computation of wall tension in a uniform wall, as originally formulated in the TriSeg model [4], which represents the three ventricular walls enclosing two cavities.

C.1 The original CircAdapt model

The one-fiber model of [5] describes a pressurized cavity enclosed by a wall composed of fibers embedded in a soft incompressible material. Within the CircAdapt framework, this model is evaluated at the mid-wall level.

An actively contracting chamber $c \in \{\mathrm{LV}, \mathrm{RV}, \mathrm{LA}, \mathrm{RA}\}$ is described by the state variables cavity volume V_c, contractile element length of the sarcomere L_c^{cont}, and contractility C_c (S21). Blood inflow and outflow induce changes in cavity volume V_c, which in turn determine cavity pressure.

In the original CircAdapt model [6], cavity pressures are derived from cavity volumes as follows. The cavity volume V_c determines the mid-wall area A_c^{mid}, defined as the surface dividing the wall volume in two equal parts along the radial direction. The mid-wall volume is given by

$$V_c^{\mathrm{mid}} = V_c + \frac{1}{2} V_c^{\mathrm{wall}}, \tag{S1}$$

where V_c^{wall} denotes the wall volume.

Chambers are approximated as spheres, leading to the following relations between volume and surface:

$$C_c^{\mathrm{mid}} = \left(\frac{4\pi}{3V_c^{\mathrm{mid}}} \right)^{1/3}, \tag{S2}$$

$$A_c^{\mathrm{mid,tot}} = \frac{4\pi}{\left(C_c^{\mathrm{mid}}\right)^2}, \tag{S3}$$

$$A_c^{\mathrm{mid}} = A_c^{\mathrm{mid,tot}} - A_c^{\mathrm{mid,dead}}, \tag{S4}$$

where C_c^{mid} is the mid-wall curvature (inverse radius), and $A_c^{\mathrm{mid,dead}}$ represents the non-contractile area (e.g., valve orifices).

The mid-wall area determines the myofiber strain. The natural fiber strain E_c^{fib} is computed as

$$E_c^{\mathrm{fib}} = \frac{1}{2} \ln \left(\frac{A_c^{\mathrm{mid}}}{A_c^{\mathrm{mid,ref}}} \right), \tag{S5}$$

where $A_c^{\mathrm{mid,ref}}$ is the reference mid-wall area, computed from (S4) using reference values of the volumes.

Given the fiber strain, a constitutive model is used to compute the corresponding myofiber stress σ_c^{fib}. This stress drives the wall tension. In CircAdapt, the relation between mid-wall tension T_c^{mid}, mid-wall area A_c^{mid}, and fiber stress is derived from conservation of energy:

$$T_c^{\mathrm{mid}} \, \mathrm{d}A_c^{\mathrm{mid}} = \sigma_c^{\mathrm{fib}} V_c^{\mathrm{wall}} \, \mathrm{d}E_c^{\mathrm{fib}}. \tag{S6}$$

Using (S5), this yields

$$T_c^{\mathrm{mid}} = \frac{\sigma_c^{\mathrm{fib}} V_c^{\mathrm{wall}}}{2A_c^{\mathrm{mid}}}. \tag{S7}$$

In the TriSeg model [4], the geometries of the three ventricular walls are iteratively adjusted to satisfy mechanical equilibrium at their junction. As a result, wall areas A_c^{mid} and curvatures C_c^{mid} evolve during the iteration. Once wall tension and curvature are known, the transmural pressure is computed via Laplace's law:

$$p_c^{\mathrm{trans}} = 2T_c^{\mathrm{mid}} C_c^{\mathrm{mid}}. \tag{S8}$$

Cavity pressure is then obtained by adding the pericardial pressure:

$$p_c = p_c^{\mathrm{trans}} + p_{\mathrm{peri}}.$$

Cavity pressures are subsequently used to update flows across valves and, consequently, cavity volumes.

To account for intraventricular and transventricular heterogeneity in activation and deformation, we adopt the MultiPatch approach [7].

C.2 The MultiPatch model

Let us consider a wall subdivided into n patches. To simplify notation, cavity-related variables are denoted without subscripts (e.g., V for cavity volume), whereas quantities indexed by j refer to the j-th patch. In particular, V_j and A_j^{ref} denote the patch volume and reference area, respectively. The superscript "mid" is omitted for brevity.

In this formulation, stress and strain are allowed to vary across patches, and therefore Eq. (S7) no longer holds uniformly over the wall. To solve the resulting equilibrium problem, the wall tension T is linearized around a reference configuration corresponding to the wall area at zero tension, denoted by A_0:

$$T(A) \approx \frac{\mathrm{d}T}{\mathrm{d}A}(A - A_0). \tag{S9}$$

For each patch, an analogous linearized relation is introduced:

$$T_j(A_j) \approx \frac{\mathrm{d}T_j}{\mathrm{d}A_j}(A_j - A_{0,j}), \tag{S10}$$

where $A_{0,j}$ is the zero-tension area of patch j.

Since transmural pressure and curvature are common to all patches within a wall, Laplace's law implies that the wall tension is uniform, i.e., $T_j = T$ for all patches. When the wall tension vanishes, the total mid-wall area equals the sum of the zero-tension areas of all patches:

$$A_0 = \sum_{j=1}^{n} A_{0,j}. \tag{S11}$$

Differentiating Eq. (S11) with respect to T and inverting yields:

$$\frac{\mathrm{d}T}{\mathrm{d}A} = \frac{1}{\sum_{j=1}^{n} \left(\frac{\mathrm{d}T_j}{\mathrm{d}A_j}\right)^{-1}}, \tag{S12}$$

which defines the effective wall stiffness.

Equations (S11) and (S12) are then used in Eq. (S9) to determine the wall tension T for a given wall area A within the TriSeg iterative scheme. Once the TriSeg solution is obtained, the transmural pressure p_c^{trans} is computed using Laplace's law (S8).

Given the wall tension, the patch areas A_j are recovered from Eq. (S10). The fiber strain E_j^{fib} is then computed for each patch using the patch-wise equivalent of Eq. (S5), and the corresponding fiber stress σ_j^{fib} is obtained from the sarcomere model (Appendix C.3). Different activation times are assigned to each patch, resulting in heterogeneous stress and strain distributions.

To evaluate Eqs. (S11) and (S12), the zero-tension areas $A_{0,j}$ and patch stiffnesses $\frac{\mathrm{d}T_j}{\mathrm{d}A_j}$ must be computed. Assuming spherical geometry and isotropic deformation, the patch area satisfies:

$$A_j = \left(\frac{L_j^{\mathrm{s}}}{L_j^{\mathrm{s,ref}}}\right) A_j^{\mathrm{ref}}, \tag{S13}$$

where L_j^{s} is the sarcomere length and $L_j^{\mathrm{s,ref}}$ its reference value.

Since L_j^{s} is not directly available during the TriSeg iteration, an initial estimate is obtained using the contractile element length L_j^{cont} (see Appendix C.3), yielding:

$$E_{j,i}^{\mathrm{fib}} = \ln\left(\frac{L_j^{\mathrm{cont}}}{L_j^{\mathrm{s,ref}}}\right). \tag{S14}$$

From this estimate, the sarcomere model provides the corresponding fiber stress $\sigma_{j,i}^{\mathrm{fib}}$ and stiffness $\frac{\mathrm{d}\sigma_{j,i}^{\mathrm{fib}}}{\mathrm{d}E_{j,i}^{\mathrm{fib}}}$. The induced patch tension is then given by

$$T_{j,i} = \frac{\sigma_{j,i}^{\mathrm{fib}} V_j}{2A_{j,i}}, \tag{S15}$$

where $A_{j,i}$ is the estimated patch area.

The patch stiffness follows as

$$\frac{\mathrm{d}T_{j,i}}{\mathrm{d}A_{j,i}} = \left(\frac{\mathrm{d}\sigma^{\mathrm{fib}}_{j,i}}{\mathrm{d}E^{\mathrm{fib}}_{j,i}} - 2\sigma^{\mathrm{fib}}_{j,i} \right) \frac{V_j}{4A^2_{j,i}}. \tag{S16}$$

Finally, the zero-tension area is obtained from Eq. (S10):

$$A_{0,j} = A_{j,i} - \frac{T_{j,i}}{\mathrm{d}T_{j,i}/\mathrm{d}A_{j,i}}. \tag{S17}$$

C.3 Sarcomere mechanics

In this section, we describe the sarcomere module of CircAdapt as introduced in the original model [6], where the subscript c denotes the cavity. In the MultiPatch formulation, the cardiac wall is subdivided into N patches, so that each variable indexed by c gives rise to N patch-specific equations, allowing mechanical parameters to vary across patches.

A sarcomere is modeled using a three-element Hill-type contraction model [8]. The contractile element, with length L_c^{cont}, is arranged in series with an elastic element of length L_c^{elast}, and this series combination is in parallel with an additional elastic element. The total sarcomere length is given by

$$L_c^{\mathrm{s}} = L_c^{\mathrm{elast}} + L_c^{\mathrm{cont}} = L_c^{\mathrm{s,ref}} \exp\left(E_c^{\mathrm{fib}}\right), \tag{S18}$$

where $L_c^{\mathrm{s,ref}}$ is the reference sarcomere length corresponding to the reference wall area, and E_c^{fib} is the natural myofiber strain, defined as

$$E_c^{\mathrm{fib}} = \ln\left(\frac{L_c^{\mathrm{s}}}{L_c^{\mathrm{s,ref}}}\right). \tag{S19}$$

Sarcomere active stress The contractile element length L_c^{cont} evolves over time according to

$$\dot{L}_c^{\mathrm{cont}} = \frac{\mathrm{d}L_c^{\mathrm{cont}}}{\mathrm{d}t} = v^{\max}\left[\frac{L_c^{\mathrm{s}} - L_c^{\mathrm{cont}}}{L^{\mathrm{elast,iso}}} - 1\right], \tag{S20}$$

where $L^{\mathrm{elast,iso}}$ is the length of the series elastic element during isovolumetric contraction, and $v^{\max}$ is the maximum contraction velocity.

Active stress also depends on time through the contractility variable C_c, a phenomenological quantity representing the density of cross-bridges within the sarcomere. Contractility increases upon activation and exhibits a rise and decay phase with distinct time constants. The rate of increase depends on sarcomere length [9]. Active stress increases with contractility, contractile element length, and series elastic element stretch.

The evolution of contractility is modeled as

$$\dot{C}_c = f_c^{\mathrm{rise}}(t) C_c^{\mathrm{s}}\left(L_c^{\mathrm{cont}}\right) - f_c^{\mathrm{decay}}(t) C_c. \tag{S21}$$

The rise function f_c^{rise} describes the formation of cross-bridges:

$$f_c^{\mathrm{rise}}(t) = \frac{1}{t_c^{\mathrm{rise}}} 0.02\, x_c^3 (8 - x_c)^2 \exp(-x_c), \tag{S22}$$

$$x_c(t) = \min\left(8, \max\left(0, \frac{t - t_c^{\mathrm{act}}}{t_c^{\mathrm{rise}}}\right)\right), \tag{S23}$$

where t_c^{act} is the activation onset time and

$$t_c^{\mathrm{rise}} = 0.55\, \tau^{\mathrm{R}}\, t_c^{\mathrm{act,ref}}.$$

The activation time t_c^{act} is defined relative to the beginning of the cardiac cycle t^{bt}:

$$t^{\mathrm{bt}} = n\, t_{\mathrm{cycle}}, \tag{S24}$$

such that

$$t_c^{\mathrm{act}} = t^{\mathrm{bt}} \tag{S25}$$

for the atria, and

$$t_c^{\mathrm{act}} = t^{\mathrm{bt}} + t^{\mathrm{AV}} + \Delta t_c^{\mathrm{act}} \tag{S26}$$

for the ventricles, where $\Delta t_c^{\mathrm{act}}$ is the patch-wise activation delay from the EP model and t^{AV} is the atrioventricular delay.

The decay of contractility is governed by

$$f_c^{\mathrm{decay}}(t) = \frac{1}{2t_c^{\mathrm{decay}}}\left[1 + \sin\left(\mathrm{sign}(y_c)\min\left(\frac{\pi}{2}, |y_c|\right)\right)\right],$$
$$y_c(t) = \frac{t - t_c^{\mathrm{act}} - t_c^{\mathrm{act,dur}}}{t_c^{\mathrm{decay}}},$$

with

$$t_c^{\mathrm{decay}} = 0.33\,\tau^{\mathrm{D}}\,t_c^{\mathrm{act,ref}},$$

and contraction duration

$$t_c^{\mathrm{act,dur}} = (0.65 + 1.0570\,L_c^{\mathrm{norm}})\,t_c^{\mathrm{act,ref}}.$$

Here, the normalized sarcomere length is defined as

$$L_c^{\mathrm{norm}} = \max\left(0.0001, \frac{L_c^{\mathrm{cont}}}{L^{\mathrm{act0,ref}}} - 1\right),$$

where $L^{\mathrm{act0,ref}}$ is the sarcomere length at zero active stress.

The function C_c^{s} accounts for the dependence of cross-bridge formation on sarcomere length:

$$C_c^{\mathrm{s}}\left(L_c^{\mathrm{cont}}\right) = \tanh\left(0.75 \cdot 9.1204\,(L_c^{\mathrm{norm}})^2\right).$$

Finally, the active fiber stress is given by

$$\sigma_c^{\mathrm{fib,act}} = L^{\mathrm{act0,ref}}\,\sigma^{\mathrm{act,max}}\,C_c\,L_c^{\mathrm{norm}}\frac{L_c^{\mathrm{s}} - L_c^{\mathrm{cont}}}{L^{\mathrm{elast,iso}}}, \tag{S27}$$

where $\sigma^{\mathrm{act,max}}$ is the maximum isometric active stress.

Sarcomere passive stress The passive stress $\sigma_c^{\mathrm{fib,pas}}$ is modeled as the sum of two contributions,

$$\sigma_c^{\mathrm{fib,pas}} = \sigma_c^{\mathrm{fib,tit}} + \sigma_c^{\mathrm{fib,ecm}}, \tag{S28}$$

representing the stresses generated by intracellular structures (primarily titin, a key structural protein of the sarcomere anchored to the Z-disc) and by the extracellular matrix (ECM), respectively.

Both components depend on the passive fiber stretch, defined as

$$\lambda_c^{\mathrm{pas}} = \frac{L_c^{\mathrm{s}}}{L^{\mathrm{pas0,ref}}},$$

where $L^{\mathrm{pas0,ref}}$ is the sarcomere length at zero passive stress and L_c^{s} is the total sarcomere length.

The titin contribution is modeled as

$$\sigma_c^{\mathrm{fib,tit}} = 0.01\,\sigma^{\mathrm{act,max}}\left(\lambda_c^{\mathrm{pas}\,k^{\mathrm{tit}}} - 1\right),$$

where $\sigma^{\mathrm{act,max}}$ is the maximal isometric stress, and the exponent k^{tit} is defined as

$$k^{\mathrm{tit}} = 2\frac{L^{\mathrm{s,ref}}}{L^{\mathrm{s,pas}}},$$

where $L^{\mathrm{s,pas}}$ is a characteristic length scale governing passive stiffness.

The ECM contribution is modeled as a stiffer nonlinear response:

$$\sigma_c^{\mathrm{fib,ecm}} = 0.0349\,\sigma^{\mathrm{pas,max}}\left(\lambda_c^{\mathrm{pas}\,10} - 1\right), \tag{S29}$$

where $\sigma^{\mathrm{pas,max}}$ is an empirical parameter.

Sarcomere total stress The total myofiber stress σ_c^{fib} is given by the sum of the active stress (S27) and the passive stress (S28):

$$\sigma_c^{\text{fib}} = \sigma_c^{\text{fib,act}} + \sigma_c^{\text{fib,pas}}. \tag{S30}$$

The sarcomere stiffness κ_c^{fib} is defined as the derivative of total fiber stress with respect to fiber strain:

$$\kappa_c^{\text{fib}} = \frac{\partial \sigma_c^{\text{fib}}}{\partial E_c^{\text{fib}}} = \frac{\partial \sigma_c^{\text{fib,act}}}{\partial E_c^{\text{fib}}} + \frac{\partial \sigma_c^{\text{fib,pas}}}{\partial E_c^{\text{fib}}}, \tag{S31}$$

where

$$\frac{\partial \sigma_c^{\text{fib,act}}}{\partial E_c^{\text{fib}}} = L^{\text{act0,ref}}\, \sigma^{\text{act,max}}\, C_c\, L_c^{\text{norm}} \frac{L_c^{\text{s}}}{L^{\text{elast,iso}}},$$
$$\frac{\partial \sigma_c^{\text{fib,pas}}}{\partial E_c^{\text{fib}}} = 0.01\, k^{\text{tit}}\, \sigma^{\text{act,max}} \lambda_c^{\text{pas}\, k^{\text{tit}}} + 0.0349 \cdot 10\, \sigma^{\text{pas,max}} \lambda_c^{\text{pas}\, 10}.$$

C.4 Vessel module

The tube module represents compliant blood vessels capable of propagating pressure–flow waves superimposed on a mean flow [6]. Vessels directly connected to the heart, namely the aorta (AO), pulmonary artery (AP), venae cavae (VC), and pulmonary veins (VP), are modeled using this formulation.

The lumen cross-sectional area is computed as

$$A_t = \frac{V_t}{l_t}, \tag{S32}$$

where V_t is the vessel volume and l_t is the segment length.

Using a fibrous tube model [5], the average fiber stretch λ_t is given by

$$\lambda_t = \left(1 + \frac{2V_t}{V_t^{\text{wall}}}\right)^{1/3} = \left(1 + \frac{2A_t}{A_t^{\text{wall}}}\right)^{1/3}, \tag{S33}$$

where A_t^{wall} is the wall cross-sectional area and $V_t^{\text{wall}} = A_t^{\text{wall}} l_t$ is the wall volume.

The vessel pressure depends on the stretch λ_t as

$$p_t = \sigma_t(\lambda_t)\, \lambda_t^{-3}, \tag{S34}$$

where σ_t is the mean Cauchy fiber stress, modeled by the constitutive law

$$\sigma_t(\lambda_t) = \sigma_t^{\text{ref}} \left(\frac{\lambda_t}{\lambda_t^{\text{ref}}}\right)^{k_t}. \tag{S35}$$

Here, k_t is a stiffness exponent, λ_t^{ref} is the reference fiber stretch,

$$\lambda_t^{\text{ref}} = \left(1 + \frac{2V_t^{\text{ref}}}{V_t^{\text{wall}}}\right)^{1/3},$$

and σ_t^{ref} is the corresponding reference stress,

$$\sigma_t^{\text{ref}} = p_t^{\text{ref}} \left(\lambda_t^{\text{ref}}\right)^3,$$

with p_t^{ref} denoting the reference pressure.

Combining the above relations yields the current vessel pressure:

$$p_t = p_t^{\text{ref}} \left(\frac{A_t^{\text{wall}} + 2A_t}{A_t^{\text{wall}} + 2A_t^{\text{ref}}}\right)^{\frac{k_t - 3}{3}}, \tag{S36}$$

where A_t^{ref} is the reference cross-sectional area and $V_t^{\text{ref}} = A_t^{\text{ref}} l_t$ is the reference vessel volume.

C.5 Periphery

The pulmonary (pulm) and systemic (sys) periphery are modeled as resistive elements. The current pressure drop Δp_{py}, for $py \in \{\text{pulm}, \text{sys}\}$, is defined as the difference between the pressure in the inflow artery p_t^{prox} and that in the outflow vein p_t^{dist}:

$$\Delta p_{py} = p_t^{\text{prox}} - p_t^{\text{dist}}. \tag{S37}$$

The corresponding resistances are computed as

$$R_{py} = \frac{\Delta p_{py}^{\text{ref}}}{q^{\text{rest}}}, \tag{S38}$$

where $\Delta p_{py}^{\text{ref}}$ is the reference arteriovenous pressure drop and q^{rest} is the mean systemic flow at rest.

The resulting flow through the peripheral circulation is then given by

$$q_{py} = \frac{\Delta p_{py}}{R_{py}}. \tag{S39}$$

D CircAdapt Global Sensitivity Analysis

A global sensitivity analysis (GSA) was performed on the CircAdapt model to identify the input parameters that most strongly influence the six target output volumes. The set of model parameters considered in the analysis is reported in Table 6.

After fixing patient-specific inputs (highlighted in gray in Table 6), the GSA was conducted separately for each patient. The resulting total Sobol indices are shown in Figure S3. Each parameter was varied within predefined physiological ranges around its baseline value (see Table 6), consistent with values reported in [7].

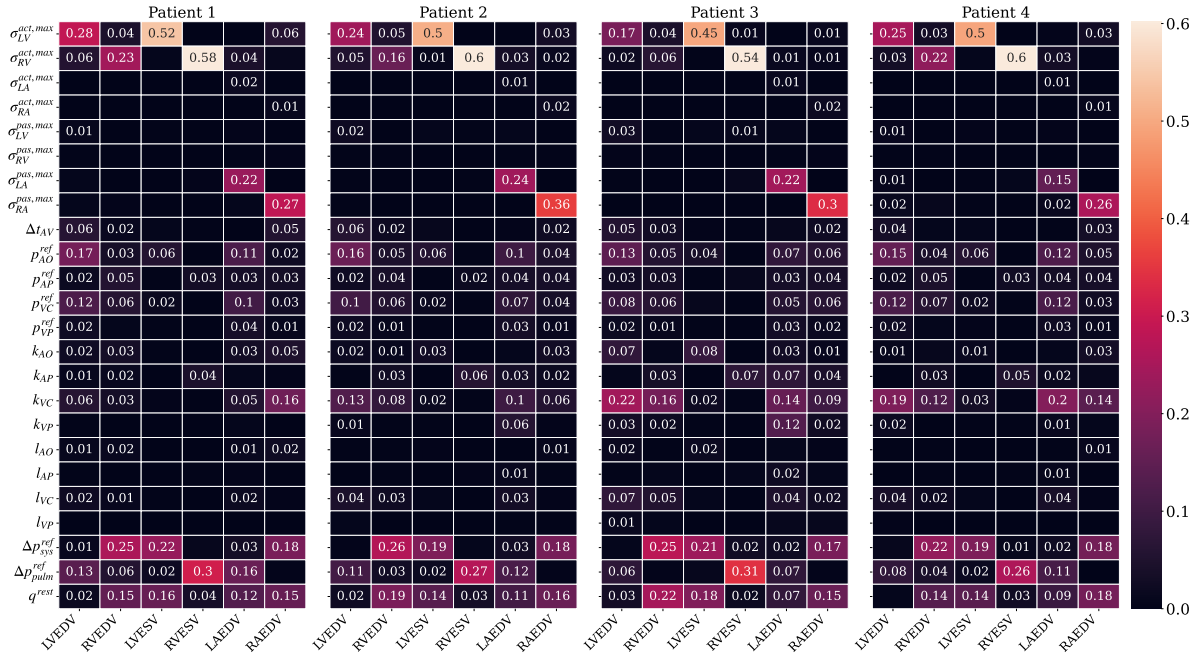

Figure S3: Heatmap of total Sobol indices obtained from the global sensitivity analysis for the four patients.

References

1. On Myocardial Segmentation, A. H. A. W. G. *et al.* Standardized myocardial segmentation and nomenclature for tomographic imaging of the heart: a statement for healthcare professionals from the Cardiac Imaging Committee of the Council on Clinical Cardiology of the American Heart Association. *Circulation* **105,** 539–542 (2002).

2. Bayer, J. *et al.* Universal ventricular coordinates: A generic framework for describing position within the heart and transferring data. *Medical image analysis* **45,** 83–93 (2018).

3. Paun, B., Bijnens, B., Iles, T., Iaizzo, P. A. & Butakoff, C. Patient independent representation of the detailed cardiac ventricular anatomy. *Medical image analysis* **35,** 270–287 (2017).

4. Lumens, J., Delhaas, T., Kirn, B. & Arts, T. Three-wall segment (TriSeg) model describing mechanics and hemodynamics of ventricular interaction. *Annals of biomedical engineering* **37,** 2234–2255 (2009).

5. Arts, T., Bovendeerd, P., Prinzen, F. W. & Reneman, R. S. Relation between left ventricular cavity pressure and volume and systolic fiber stress and strain in the wall. *Biophysical journal* **59,** 93–102 (1991).

6. Arts, T., Delhaas, T., Bovendeerd, P., Verbeek, X. & Prinzen, F. W. Adaptation to mechanical load determines shape and properties of heart and circulation: the CircAdapt model. *American Journal of Physiology-Heart and Circulatory Physiology* **288,** H1943–H1954 (2005).

7. Walmsley, J. *et al.* Fast simulation of mechanical heterogeneity in the electrically asynchronous heart using the multipatch module. *PLoS computational biology* **11,** e1004284 (2015).

8. Fung, Y.-C. Mathematical representation of the mechanical properties of the heart muscle. *Journal of biomechanics* **3,** 381–404 (1970).

9. Kentish, J. C., Ter Keurs, H., Ricciardi, L., Bucx, J. & Noble, M. Comparison between the sarcomere length-force relations of intact and skinned trabeculae from rat right ventricle. Influence of calcium concentrations on these relations. *Circulation research* **58,** 755–768 (1986).